Biomicrofluidics ARTICLE scitation.org/journal/bmf

Universal pre-mixing dry-film stickers capable of retrofitting existing microfluidics

Cite as: Biomicrofluidics **17**, 014104 (2023); doi: 10.1063/5.0122771
Submitted: 25 August 2022 · Accepted: 12 December 2022 ·
Published Online: 17 January 2023

P. Delgado,[1,2] O. Oshinowo,[1,2] M. E. Fay,[1,2] C. A. Luna,[1,2] A. Dissanayaka,[1,2] P. Dorbala,[1,2] A. Ravindran,[1,2] L. Shen,[1,2] and D. R. Myers[1,2,3,a)]

AFFILIATIONS

[1]The Wallace H. Coulter Department of Biomedical Engineering, Georgia Institute of Technology and Emory University, Atlanta, Georgia 30332, USA
[2]Department of Pediatrics, Division of Pediatric Hematology/Oncology, Aflac Cancer Center and Blood Disorders Service of Children's Healthcare of Atlanta, Emory University School of Medicine, Atlanta, Georgia 30322, USA
[3]Parker H. Petit Institute of Bioengineering and Bioscience, Georgia Institute of Technology, Atlanta, Georgia 30332, USA

[a)]**Author to whom correspondence should be addressed:** david.myers@emory.edu

ABSTRACT

Integrating microfluidic mixers into lab-on-a-chip devices remains challenging yet important for numerous applications including dilutions, extractions, addition of reagents or drugs, and particle synthesis. High-efficiency mixers utilize large or intricate geometries that are difficult to manufacture and co-implement with lab-on-a-chip processes, leading to cumbersome two-chip solutions. We present a universal dry-film microfluidic mixing sticker that can retrofit pre-existing microfluidics and maintain high mixing performance over a range of Reynolds numbers and input mixing ratios. To attach our pre-mixing sticker module, remove the backing material and press the sticker onto an existing microfluidic/substrate. Our innovation centers around the multilayer use of laser-cut commercially available silicone-adhesive-coated polymer sheets as microfluidic layers to create geometrically complex, easy to assemble designs that can be adhered to a variety of surfaces, namely, existing microfluidic devices. Our approach enabled us to assemble the traditional yet difficult to manufacture "F-mixer" in minutes and conceptually extend this design to create a novel space-saving spiral F-mixer. Computational fluid dynamic simulations and experimental results confirmed that both designs maintained high performance for $0.1 < Re < 10$ and disparate input mixing ratios of 1:10. We tested the integration of our system by using the pre-mixer to fluorescently tag proteins encapsulated in an existing microfluidic. When integrated with another microfluidic, our pre-mixing sticker successfully combined primary and secondary antibodies to fluorescently tag micropatterned proteins with high spatial uniformity, unlike a traditional pre-mixing "T-mixer" sticker. Given the ease of this technology, we anticipate numerous applications for point-of-care devices, microphysiological-systems-on-a-chip, and microfluidic-based biomedical research.

INTRODUCTION

When integrated into lab-on-a-chip devices, microfluidic mixers have the potential to automate many laboratory steps including dilutions, extractions, the addition of reagents or drugs, and particle synthesis.[1–7] To that end, numerous stand-alone, highly efficient microfluidic mixers have utilized clever design principles to overcome diffusion limitations that hinder microscale mixing.[8–10] In all cases, increasing the geometric complexity of the device enhances mixing through various mechanisms including inducing transverse flows, chaotic advection,[11] or folding flows via splitting and recombing.[12] Unfortunately, increased fabrication complexity typically accompanies the increased geometric complexity of these devices in the form of more complex soft lithography molds or multilayer assembly processes that can be difficult to co-implement with other lab-on-a-chip processes.[13,14]

Using current approaches, it remains more practical to integrate geometrically complex mixers into lab-on-a-chip devices as a stand-alone component.[15] This multi-chip approach makes biomedical research with microdevices more cumbersome and complicates translational efforts for point-of-care devices. New methods, such as 3D printing,[16,17] have shown excellent potential toward improving the manufacturability of integrated microfluidic devices.

However, more work is needed to reduce the long print times and significant process optimization for reproducible results. To complement existing fabrication and 3D printing approaches, we present an easy to manufacture a microfluidic pre-mixing sticker that seamlessly retrofits existing microfluidics without tubing and with no change to the device footprint.

Our work builds on the excellent advancements of others using dry-film adhesive tape technology. Dry-film adhesives have been used to micropattern and deposit materials;[18] create devices between glass,[19,20] wax,[21] and polymers;[22,23] create pneumatic valves in 3D fluidics;[24] and facilitate cell culture;[25] and as an intermediary layer to seal channels.[26,27] This work leverages several key advantages of dry film adhesives including simple patterning with craft and laser cutters[28] and adhesiveness to many surfaces.[29,30] Innovative applications of using dry film adhesives for creating freestanding microfluidics exist,[31,32] including using these adhesives to simplify the mixing manufacturing process.[33] Building on this work, we show that silicone dry film adhesives can easily add multi-layer high efficiency upstream and downstream processes to existing microfluidics.

Our upstream and downstream devices are essentially microfluidic "stickers" that can be peeled from a backing and applied to nearly any surface with instantaneous bonding, akin to stickers used for labels, signs, and amusement. Our approach, with a larger feature size set by the minimum line width of the laser cutter, complements the other creative implementations of sticker-like properties for microfluidics capable of smaller sized features.[34,35] This approach also decouples the fabrication process for the upstream or downstream component from the main device and offers an alternative path to monolithic integration.

As each layer of the dry-film adhesive readily sticks to itself and other surfaces, it greatly simplifies the manufacture of geometrically complex microfluidic mixers and other structures. This enables rapid fabrication of multilayer, geometrically complex, microfluidic structures while circumventing the need for complex alignment processes, varying ratios of polydimethylsiloxane (PDMS) polymers,[36] integrated photoresist/PDMS processes,[37] spun layers of PDMS,[38] surface treatments,[39] heat-mediated thermoplastic bonding,[40] and more. For example, the well-regarded F-mixer[12] can be adapted to a sticker format and assembled in minutes [Fig. 1(a)]. Building on this simple fabrication process, we now introduce a highly efficient "spiral F-mixer," a 12-layer, small footprint device that can still be assembled in minutes [Fig. 1(b)]. As mentioned, both stickers conform onto flexible surfaces [Fig. 1(c)] or retrofit existing microfluidics [Fig. 1(d)].

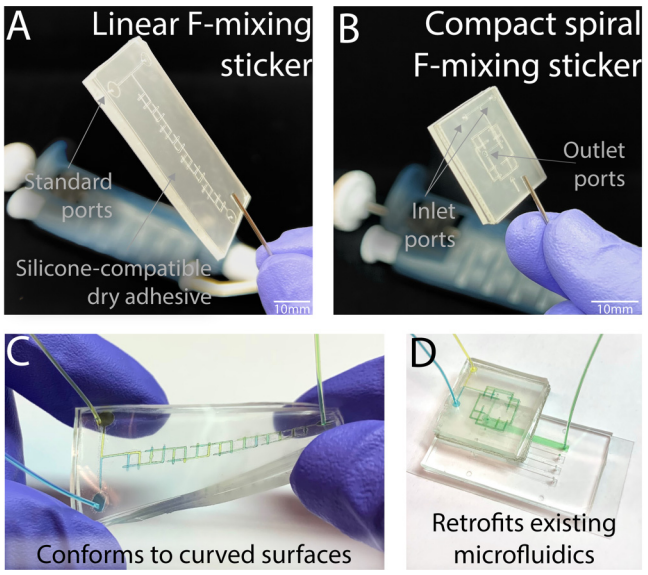

FIG. 1. The versatile novel pre-mixing microfluidic stickers can be attached to any surface, including pre-existing microfluidics. (a) Classic linear and (b) novel compact spiral F-mixing sticker designs shown with standard inlet and outlet ports. (c) Stickers are capable of conforming to curved surfaces when using a PDMS layer as the base. (d) Due to the silicone-compatible dry adhesive, the sticker is able to seamlessly retrofit existing microfluidics to implement an on the spot mixing step where necessary. In this configuration, the outlet port of the pre-mixing sticker aligns with the inlet port of the retrofitted microfluidic.

METHODS AND FABRICATION

Manufacturing stickers

The roll-based silicone microfluidics were first drafted using an Adobe illustrator. In preparation for laser cutting, a non-silicone release liner (3M 5053) was layered onto the dry adhesive exposed side of 0.13 mm thick roll-based silicone dry-adhesives on a polyethylene terephthalate (PET) carrier (3M 96042). Any air bubbles between the two layers that are formed were removed by scaping the top of the release liner with a squeegee. The specific characteristics of the silicone dry-adhesive were important in that it is designed to stick to silicone surfaces unlike more commonly available double-sided tape, as acrylic dry-adhesive would not hold the same adhesive strength to PDMS. Selecting the silicone dry-adhesive allows the sticker to have a flexible PDMS roof and optionally have an existing PDMS microfluidic-based bottom layer. The combination was then used to manufacture the final pieces of the tape with a laser cutter (Universal Laser Systems VLS 4.60) to create the tape layers as shown in Figs. 2(a) and 2(b). The settings used were 0.13 mm height and −50% quality. These settings on the laser cutter prevented excessive scorching on the tape for easier cleaning and resulted in a channel width of 200 μm. Particulates were removed from the laser cut pieces of the tape via brushing off with the blunt edge of a razor blade and simple tape cleaning. A PDMS interface layer was manufactured from Sylgard 184 (Dow Inc.) at a standard 10:1 mixture of elastomer base: curing agent. After vigorously mixing for 1–2 min, the PDMS solution was degassed for 40 min and 10 g was poured into a 100 × 15 mm Petri dish. The PDMS interface layer was cured in a 65 °C oven for 3–4 h or until use. After curing, the interface layer was peeled out of the Petri dish and manually cut to the dimensions of the final sticker device. PDMS can be made in bulk beforehand to save additional time when assembling the microfluidic sticker. A catheter punch (Syneo) was used to create a 0.75 mm⌀ hole for the inlets and outlets. Once the sticker is complete, the user can select the bottom layer based off of their applications. The configurations for the linear and spiral mixers shown in Fig. 2 are for the linear mixer to be used as a traditional standalone device and the spiral mixer to

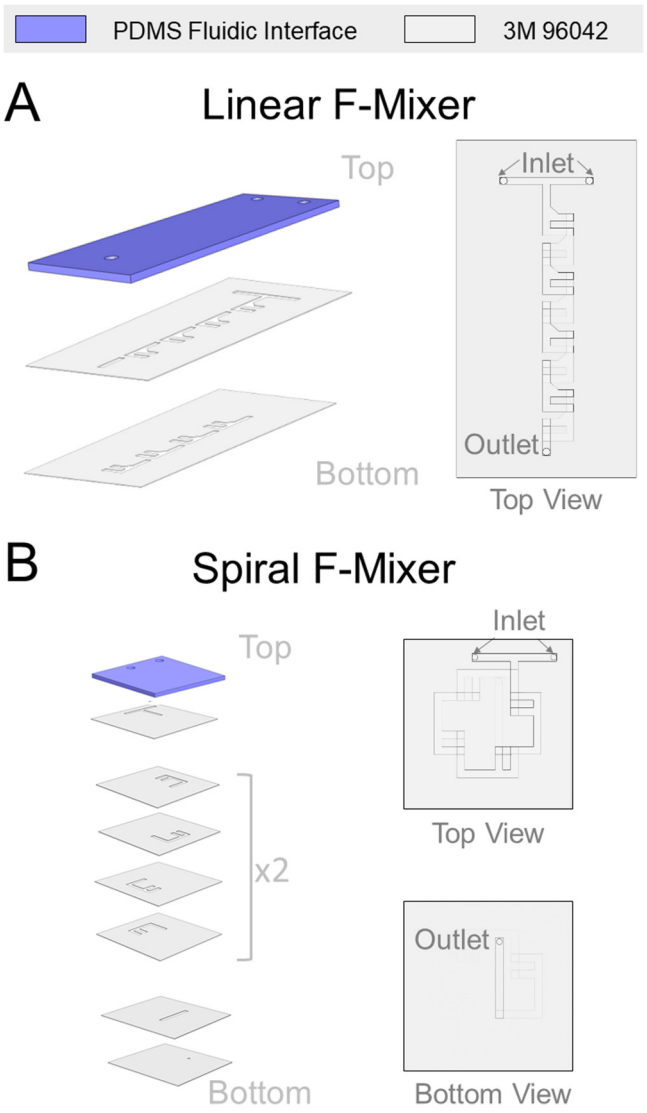

FIG. 2. Laser cut dry film tape can be layered in a straightforward manner to enable geometrically complex microfluidic stickers. (a) The linear F-mixer comprises three main layers with one PDMS fluidic interface and two layers of the 3M 96042 tape. (b) The spiral F-mixer is a space saving compact form of the linear F-mixer consisting of one PDMS fluidic interface and a total of 11 layers of the 3M 96042 tape. The final bottom layer for each microfluidic is not included in the figure but up to user preference. Linear F-mixer configuration is for standalone use, and the spiral F-mixer configuration can be adhered to existing microfluidic.

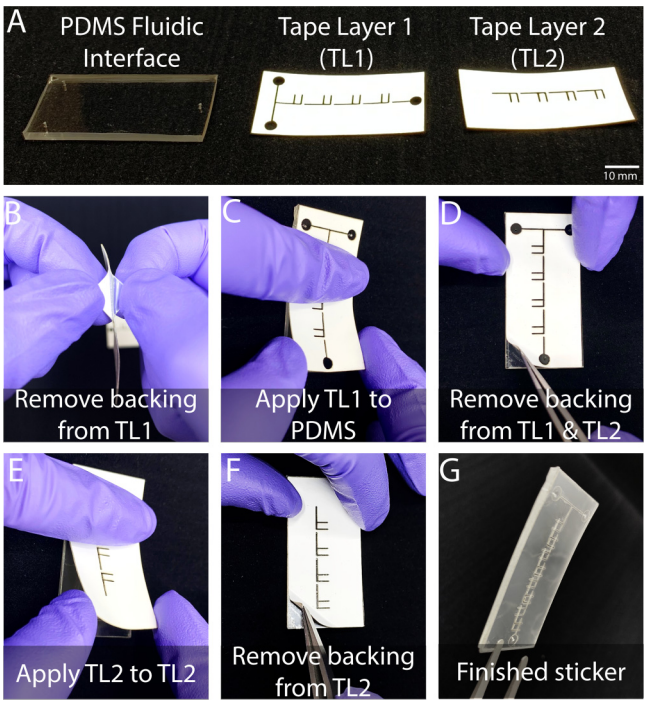

FIG. 3. Sticker microfluidics can be assembled by hand in minutes. (a) Microfluidic stickers are comprised of a fluidic interface of PDMS (Sylgard 184) with multiple laser cut tape layers. (b) Each tape layer has two backing layers that must be removed during the assembly process. (c) Upon the removal of the first backing layer, tape layer 1 can then be gently pressed onto the PDMS fluidic interface. (d) The second and final backing layer is removed from tape layer 1 with tweezers, and the first backing of tape layer 2 is removed to prepare for adhesion. (e) Tape layer 2 is applied with similar gentle pressure onto tape layer 2. (f) The final backing is removed from tape layer 2 with tweezers. (g) The microfluidic mixer manufacturing is done and ready to be applied to the user's surface of choice.

be retrofit. An additional configuration for the linear F-mixer to be compatible with being adhered to an existing microfluidic is found in Fig. 1 in the supplementary material.

The stickers are built layer by layer from the top down [Fig. 3(a)], starting with the PDMS interface layer. As shown in Fig. 3(b) for the linear F-mixer, a clear backing must be removed from the silicone tape layer before adhering it to the PDMS fluidic interface layer. Alignment was done easily by eye, as each layer was designed with tolerances to allow for minor human errors during assembly. To account for misalignment during assembly, we included tolerances that allow for a maximum misalignment of about ~1 mm for the x- and y-translational misalignment and ~3° in rotational misalignment. If a greater translational error or rotational error occurs, the channels no longer intersect with one another and the device is unable to function properly. In later designs, we also included an alignment marker consisting of a square cutout in one corner of the device (Fig. 2 in the supplementary material). Each layer is the exact same width and length as the previous layer, enabling users to align edges if preferred, akin to a deck of cards. We tested whether these tolerances were appropriate by asking five users to build three devices each. On average, the misalignment on the x-translation, y-translation, and rotational translation was 0.29 mm, 0.4 mm, and 1.88°, respectively (Table 1 in the supplementary material). In addition, all 15 devices were successfully built microfluidic, and all of the channels were able to

properly intersect and allow for fluid to flow. Because each piece has an adhesive backing, only gentle pressure is needed to attach the first tape layer to the PDMS fluidic interface layer [Fig. 3(c)]. Before attaching the second silicone tape layer, the white backing must be removed from the first tape layer [Fig. 3(d)]. The second tape layer is attached, by following similar steps, to the first one [Figs. 3(e) and 3(f)]. When adhered to the first tape layer and the PDMS layer, the linear F-mixer sticker is ready to be adhered to the user's floor layer of choice [Fig. 3(g)]. The bottom layers could consist of a traditional glass slide, PDMS, a pre-existing microfluidic or any other mixing surface of interest. The spiral F-mixer is manufactured in a similar method; however, it requires more than two pieces of silicone tape layers and a vacuum step to reduce the prevalence of bubbles blocking the channels. The F-layer of the spiral fluidic has been designed to be able to be rotated 90° and create as many layers as necessary to mix the fluid. In this paper, eight F layers for the spiral mixer were chosen for optimal mixing performance. Immediately prior to each experiment, the lone spiral mixer was placed in a vacuum chamber for at least an hour to eliminate bubbles prior to being adhered to a pre-existing microfluidic. Within seconds of removing the tape from the vacuum chamber, the spiral mixer was attached to the floor layer and 1× PBS was loaded into the channels to prime and aid in the removal of bubbles from the channels. 20 μl droplets of 1× PBS were placed at each inlet and outlet of the completed microfluidic. The adhesive bond strength for each layer is significant and difficult to pull apart manually. At the Reynolds number of 11.53, the microfluidic tape held firm for 1 h and 40 min without showing any signs of leakage. At this flow rate, we would expect any signs of failure to become apparent during this time frame, such as slight delamination. As no signs of failure were present, we anticipate that the mixer can withstand this Reynolds number for long periods of time. It was not until the mixer was brought up to the Reynolds numbers up to ~23 that the tape started to show immediate damage and exhibit the signs of leakage.

Simulated mixing performance

SolidWorks was used to create a model of the linear and spiral mixers, as shown in Fig. 2. A computational fluid dynamics (CFD) simulation was run in AutoCAD CFD on each model to generate the simulated mixing results under steady-state conditions. The diffusion coefficient characteristic of Rhodamine 6 g used for the simulations was 4×10^{-10} m^2/s.[41] The simulation was run at the standard boundary conditions of constant normal flow velocity and fixed pressures at inlets and outlets. To test the mixer's ability to create an equal mixture, the mixer was tested over a range of Reynolds numbers (0.23–11.53). This range was chosen to thoroughly characterize the sticker over a range that passive mixing devices with simple designs, such as the T-mixer, would traditionally fail over and test the highest limits for the mixer. The model was also used to simulate highly disparate mixing at Reynolds numbers 0.1, 1, and 10. The disparate mixing ratios tested were from 1:0 to 1:10, increasing by the increments of 1.

Experimental mixing performance

Experimental data were collected from the previously mentioned mixers. The equal mixing and disparate mixing were collected on a single device for the linear experiments, as well as for the spiral mixer tests. The linear mixer was run by attaching it to a coverslip, and the spiral mixer was adhered to a pre-existing microfluidic for data collection. The region of interest of the linear mixer was easy to visualize. Due to the complexity of the multiple layers on the pre-mixing spiral sticker, the region of interest was difficult to analyze so it was placed on a separate microfluidic device. No significant changes in mixing performance were expected based off of the attachment to the existing microfluidic. Multiple devices were used to collect the data for the experiments. Rhodamine B (5 g/l) diluted to 1:100 in pure DI water was mixed with pure DI water. Two 10 ml syringes were loaded with the diluted Rhodamine and DI water, one for each. The syringes were then loaded onto a syringe pump (Harvard Apparatus PhD Ultra), Tygon tubing (Cole-Parmer EW-06 419-01) was connected via a blunt needle tip, and the lines were primed prior to placing the tubing into the microfluidic. The setup was placed on the microscope stage and imaged using 3D imaging with a Nikon Ti2 and CFI Plan Apochromat Lambda 20× objective (NA 0.75). Three 3D images were taken of the end of the channel right before the outlet over the course of 5 min. The 3D images were processed and analyzed using ImageJ. The intensities of the cross sections for each 3D image were analyzed in ImageJ using the measure intensity feature and were recorded.

Evaluation of pre-mixing sticker integration

An array of pairs of fibrinogen microdots with a radius of 1.25 μm and separation of 4 μm were patterned and stamped on plasma treated coverslips (No 1.5, 24×50 mm^2) as described previously.[42,43] Briefly, the microdot pattern was created by a silicon mold using standard lithography and etching techniques. Fibrinogen (Enzyme Research Laboratory) was incubated on square ($10 \times 10 \times 3$ mm^3) polydimethylsiloxane (PDMS) at 30 μg/ml for 30 min at 37° before being rinsed with water and dried with nitrogen gas. These fibrinogen-coated PDMS squares were then placed onto the plasma-treated silicon mold in order to create the microdot-patterned PDMS "stamp." Two micropatterned "stamps" were then placed side by side onto a plasma treated 24×50 mm^2 coverslip and subsequently blocked with 1% BSA before experimentation. A simple four-channel microfluidic was laser cut from roll-based silicone to create the channels for the microfluidic and adhered to the coverslip containing the "stamp." A PDMS roof containing inlets and outlets was then placed on top of the four channel tape channels, and 1% BSA was pipetted into the channels.

To explore a functional application for the mixer, we assessed its ability to work for binding primary and secondary antibodies to fluorescently tag microdots. The spiral F-mixer was utilized to be retrofit to a pre-existing microfluidic that contained the micropatterned dots. Equal amounts of two different antibodies were flowed into the channels at a Reynolds number of 0.23. The primary antibody, mouse anti-human fibrinogen monoclonal antibody (Enzyme Research Laboratory), was mixed with 1% BSA solution (1:40). The secondary antibody, Alexa Flour 488 tagged goat anti-mouse antibody (Thermo Fisher), was mixed with 1% BSA solution (1:80). Total internal reflectance fluorescence (TIRF) microscopy was used to capture the fluorescent images of the antibodies

binding to the micropatterned dots over 20 min. The resulting images were then analyzed via a custom Python script to capture and record the increasing intensity of the dots over time using the region property analysis implemented with scikit-image.[44]

To further compare the F-mixer's efficiency against a traditional T-mixer, a T-mixer was laser cut from the same roll-based silicone used to make the F-mixers and adhered to a pre-existing microfluidic similar to that of the spiral F-mixer. The T-mixer was cut to have a similar footprint as the spiral F-mixer. An additional T-mixer that was laser cut and shared the approximate total length (70 mm) of the spiral F-mixer was also created for supplemental data. The primary antibody, sheep anti-human fibrinogen monoclonal antibody (Enzyme Research Laboratory), was mixed with 1% BSA solution (1:40). The secondary antibody, Alexa Flour 488 tagged donkey anti-sheep antibody (Thermo Fisher), was mixed with 1% BSA solution (1:80). A sheep antibody was used to assess mixing performance across different sources. The primary and secondary antibodies were flowed through the channels of the T and F mixers at a flow rate of 10 μl/min. After 5 min, the flow was stopped and the channels were flushed with 200 μl of 1× PBS three times. Fluorescent images of the antibodies binding to the microdots were then taken over the entire surface to quantify the spatial uniformity.

RESULTS

Linear and spiral F-Mixer design

The linear F-mixer design follows the traditional injection molded F-mixer design, consisting of two inlets and one outlet. As each fluid goes in through their respective inlet, the two fluids meet at the beginning of the T-mixer before being split through the first F in the series. While going through the series, the fluids will be continuously split and then recombined to ensure that mixing is not reliant only on diffusion like a "T-mixer." The spiral F-mixer represents a conceptual extension of the classic F-mixer that leverages our rapid manufacturing process. Each split and recombine process also features a 90° rotation. The layers for each F were designed to be interchangeable, and one simply rotates each subsequent layer by 90° to connect to the previous layer. This particular aspect helps simplify the design and assembly by having only four unique device layers. This 90° rotation after each split and recombine allowed for a significant reduction in the area of the device. From a design perspective, the spiral F-mixer utilizes approximately 50% less space than the linear F-mixer. Both sticker microfluidic modules are easily implemented onto virtually any surface and can be assembled in minutes. In addition, our multilayer design approach can be conceptually extended further to include more layers.

Simulations

The simulations run on AutoCAD CFD showed that the linear and spiral mixers were able to mix reliably over a range of Reynolds numbers as shown in Fig. 4. Excellent mixing performance was predicted for high (10) and low (0.1) Reynolds numbers as well as for varying volumetric ratios of inputs from 1:1 to 1:10. Beginning first with mixing equal ratios of each fluid, at a low

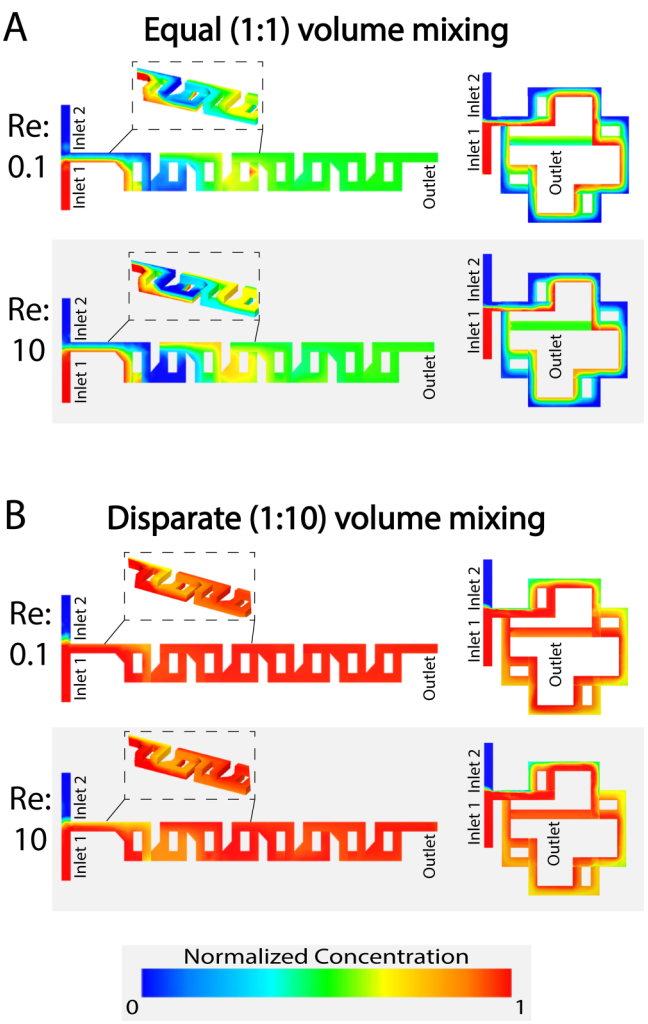

FIG. 4. Our simulations predict that both mixers will have high mixing performance for different flow rates and input volume ratios. (a) The linear and spiral F-mixing stickers are able to mix at a 1:1 ratio of equal volume mixing over low (0.1) and high (10) Reynolds numbers consistently. (b) The pre-mixing stickers are also capable of thoroughly mixing highly disparate volumes at a 1:10 ratio [low (0.1) and high (10) Reynolds numbers].

Reynolds number (Re = 0.1), the final concentrations were 0.502 and 0.514 for the linear and spiral mixers, respectively [Fig. 4(a)]. When simulated at a high Reynolds number (Re = 10), the values were 0.505 and 0.517 [Fig. 4(a)]. Both cases are close to the ideal 0.5 expected for perfect mixing. The mixer exhibited a comparable performance when mixing highly disparate volumes. When mixed at a 1:10 ratio at a low Reynolds number of 0.1, the linear mixer's concentration was 0.945 and spiral mixer's concentration was 0.929 [Fig. 4(b)]. When mixed at a high Reynolds number of 10, the linear and spiral mixers' concentrations were 0.959 and 0.929, respectively [Fig. 4(b)]. Again, this was close to the theoretical value of 0.909 that would be expected for perfect mixing.

Fluorescent dye mixing performance

Our experimental results show that the mixers have excellent performance that closely aligns with the predicted simulated results for a range of flowrates and disparate mixing ratios. To thoroughly characterize the mixing for the microfluidic, the mixer's performance was first evaluated over a range of Reynolds numbers from 2.31 to 11.53, which is a range that encompasses flow rates that would not be conducive to mixing with a traditional passive mixer. A Reynolds number of 0.02 would be needed for successful mixing with a comparatively sized (similar channel width) diffusion-based T-mixing sticker. Our results showed that the linear and spiral simulations strongly correlated with the experimental values, as shown in Fig. 5(a) for both the linear and spiral F-mixers. To continue to test the performance of the F-mixers, disparate mixing was performed via simulation and experimentally. The mixing was tested at three different conditions (Reynolds numbers 0.1, 1, and 10). At a Reynolds number of 0.1, the values very closely correlated with the simulated values [Fig. 5(b)]. As the Reynolds number increased, the mixed concentration values continued to follow the trend that was set by the simulated results with very minor deviations [Figs. 5(c) and 5(d)]. Additional simulations were run to assess whether or not the addition of adhering the sticker to an existing device would alter the mixing of the mixers. This was shown to have no significant change in the mixing efficiency (Fig. 3 in the supplementary material).

Manufacturing optimization

We found that careful and consistent pressure during assembly was key to consistent high mixing performance. The best results were achieved by a light tapping pressure applied throughout the surface of each tape layer during manufacturing. When the assembly pressure is too high, channel collapse and/or collapse of the port structures could obstruct the channels and reduce the mixing efficiency. Optimization of the laser cutting parameters to reduce burning on the edges of the tape was also essential to maintain proper mixing. Excessive burning on the edges of the channels resulted in particulates that were hard to reduce during the sticker

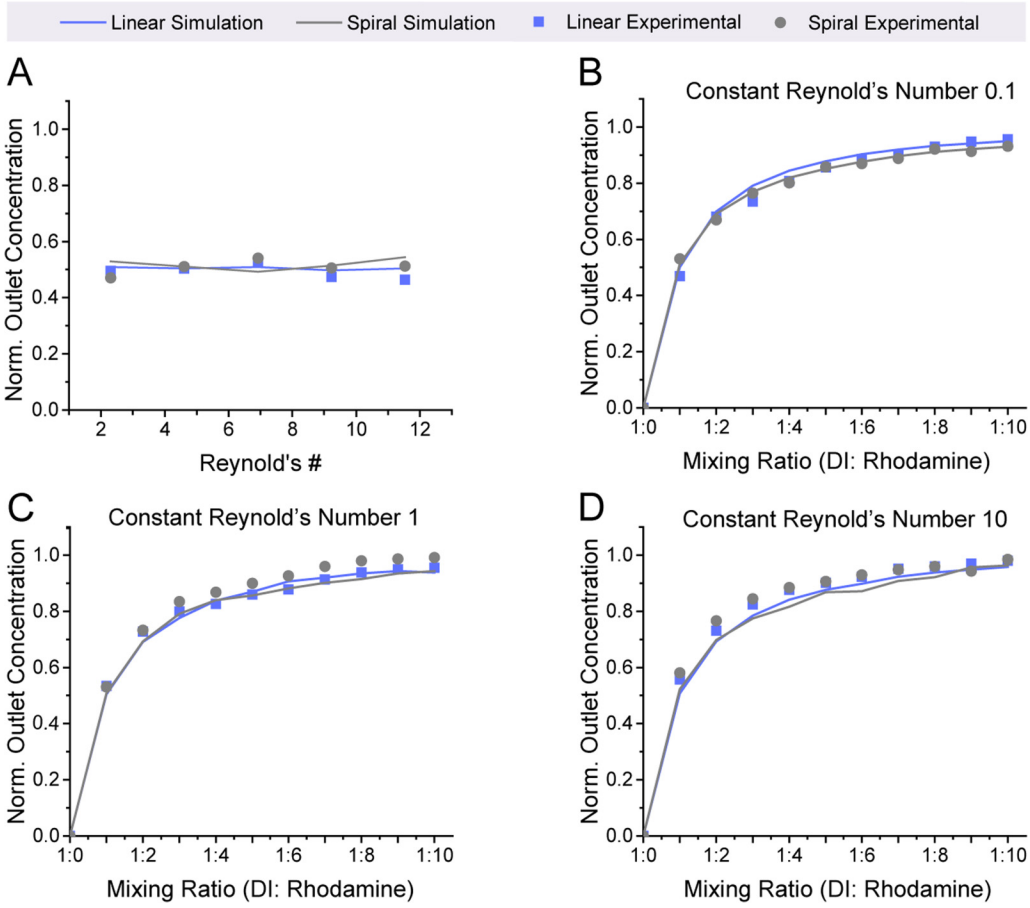

FIG. 5. Our experimental results strongly correlate with simulated predictions. (a) The mixing performance at a 1:1 input volume ratio remains steady over a wide range of Reynolds numbers (2.31–11.53). (b)–(d) The premixing sticker experimental results match with predicted values from simulations at Reynolds numbers of 0.1, 1, and 10 for a wide range of input volume ratios.

layer procedures, which would, in turn, release particulates into the downstream microfluidic and pre-mixing sticker. Throughout testing, the spiral mixer showed a non-symmetric nature, seemingly favoring one side over the other rather than showing no preference like the linear mixer, at a 10:1 ratio of splitting and mixing the steams of fluids. This resulted in minor streamlines of high and low concentrations through the channel. This was found to have negligible deviations in mixing performance, as it could be eliminated by switching the inlets that each solution would flow through. The inlet with the highest amount of volume flowing through it tended to work best when being at inlet 1, as shown in Fig. 4.

Real-time mixing of antibodies to immunofluorescently label micropatterned proteins

Mixing primary and secondary antibodies immediately prior to labeling a microstamped protein exemplifies the key strengths of our sticker-based microfluidics. The tape used for the sticker has been shown previously to be biocompatible as the tape is easily sterilized for cell culture use via being in a 120° oven for at least an hour or sterilized by blocking the channels prior to use.[45,46] The tape, also, did not disturb or alter micropatterned proteins, as shown with the initial sticker microfluidic that was adhered to the surface to create simple straight channels followed by a pre-mixing sticker [Fig. 6(a)]. The unlabeled primary antibody mixed with the labeled secondary antibody and the successful product of the mixture was shown on the microdots. As time passed and more of the antibodies continued to mix and flow through the channels, the intensity of the microdots continued to increase [Fig. 6(b)]. The microdot intensity continued to increase until the microdots were saturated with bound antibodies. The spiral F-mixer sticker was shown to easily be able to mix two antibodies and distribute the completely mixed antibodies throughout the channel.

Spatial mixing performance of immunofluorescently labeled micropatterned proteins

In addition to showing the mixer's biocompatibility and ability to pre-mix two components, we also wanted to test the spatial performance of the mixer and how well distributed these components were. For a control, we created a standard T-mixer with a similar footprint to our F-mixer, in which two streams meet and mixing is performed exclusively via diffusion. Both our spiral F-mixer and a traditional T-mixer were adhered upstream of a straight channel microfluidic, with a width of ~0.2 mm [Figs. 7(a) and 7(b)]. The results in Figs. 7(c) and 7(d) showed that at the same Reynolds number (Re = 0.23) as the spiral F-mixer, the T-mixer performance was suboptimal. This was clearly shown with a bright line in the middle of the channel showing a successful mix of the antibodies surrounded by significantly less bright microdots [Fig. 7(d)]. Dark areas on the T-mixer indicate the absence of either the primary or secondary antibody since both are needed to generate a fluorescent signal. In comparison, the spiral F-mixer outperformed the T-mixer and had a well-distributed brightness of the microdots, enabling the visualization of every protein microdot across the channel [Fig. 7(c)]. The T-mixer, also, showed about half of the fluorescent intensity when compared to the spiral F-mixer, potentially indicating that there was less successful mixing done

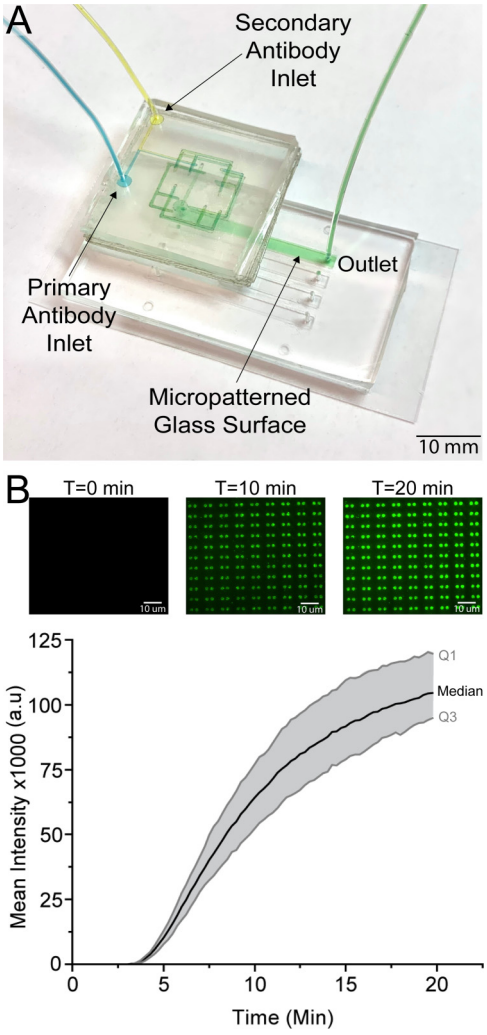

FIG. 6. A spiral pre-mixing sticker retrofitted onto an existing microfluidic successfully mixed primary and secondary antibodies to immunofluorescently stained microstamped proteins. (a) The inherently biocompatible spiral F-mixing sticker was retrofitted onto a pre-existing microfluidic device that had a microstamped protein on the bottom cover glass surface. (b) Time lapse fluorescent images show that the mix of primary and secondary antibodies was able to successfully immunofluorescently stain the microstamped proteins in an even manner to saturation over 20 min. This highlights both the successful mixing and biocompatibility of the pre-mixing sticker.

overall. A long T-mixer with similar total channel length to the spiral F-mixer was created in order to investigate the contribution of geometry to mixing. Similar to the shorter T-mixer, it was found to have half of the overall fluorescent intensity as the spiral F-mixer (Fig. 4 in the supplementary material). It is important to note that while collecting, the longer T-mixer system proved to be suboptimal and cumbersome for practical applications as the existing microfluidic and long T-mixer combination did not fit onto a traditional microscope stage meant for microscope slides. As a result,

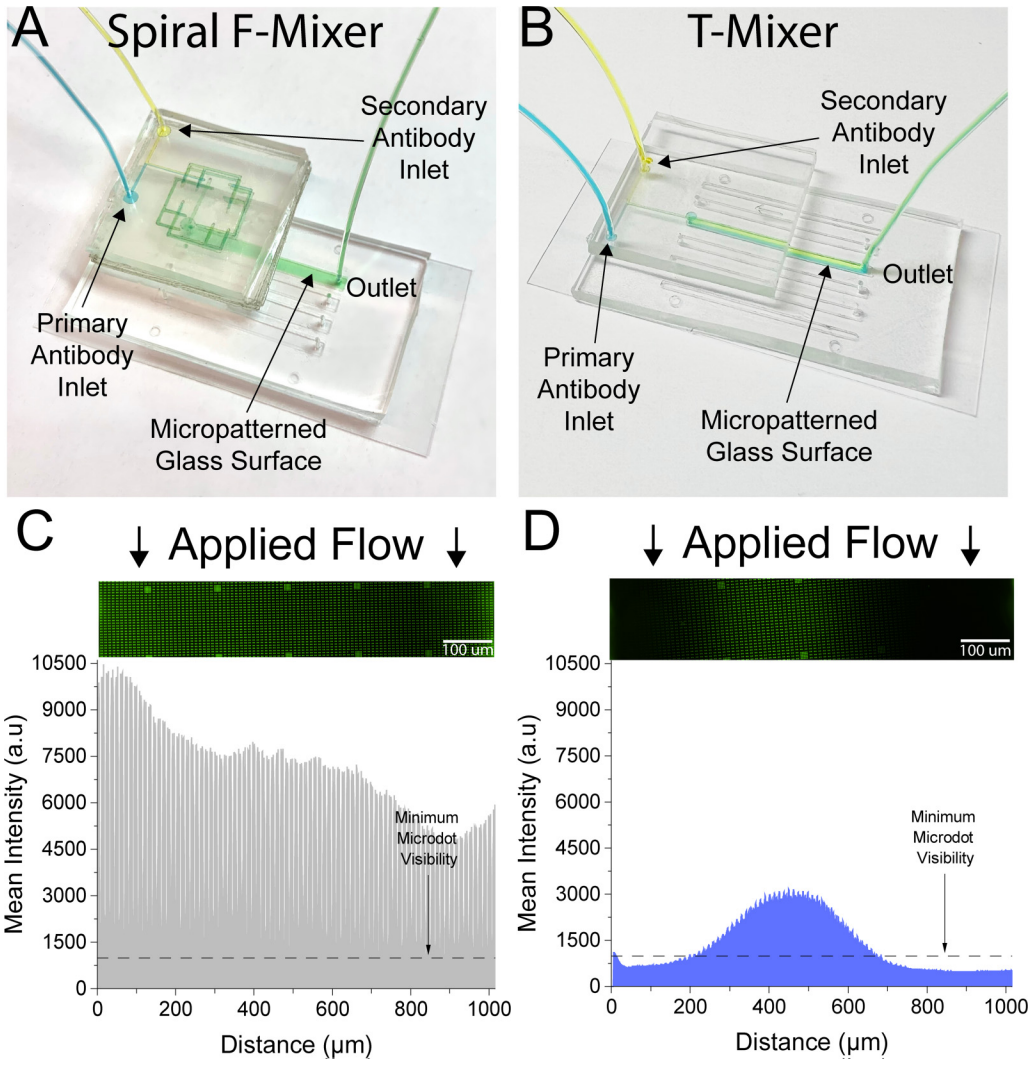

FIG. 7. The spiral F-mixer has vastly superior mixing spatial distribution as compared to a diffusion-limited T-mixer. (a) A spiral pre-mixing sticker was retrofitted onto an existing microfluidic containing micropatterned proteins. (b) The T-mixer was laser cut in the same tape material as the spiral mixing sticker and adhered onto a pre-existing microfluidic device. (c) The spiral sticker successfully mixed the primary and secondary antibodies that subsequently enabled the visualization of all patterned proteins in the channel. (d) Conversely, the T-mixer only enabled the visualization of proteins along the middle of the channel as antibody mixing was diffusion limited. For both experiments, Re = 0.23.

the mixer had to be carefully cut with a blade to be able to load the existing microfluidic onto the microscope stage and collect the data. Additionally, insufficient mixing can be seen clearly by eye when comparing the long T-mixer with the F-mixer at various Reynolds numbers (Fig. 5 in the supplementary material).

DISCUSSION

In this paper, we demonstrate a novel universal mixing sticker. The key innovation was implementing the laser-cut silicone-adhesive coated polymer sheet to create the once complex to manufacture F-mixer. The sticker not only was utilized to easily create multilayer designs, but also revamped this design by creating the first to our knowledge spiral F-mixer. The spiral F-mixer not only decreases the amount of the surface area required for the mixer, but also showcases the polymer's ability to build multilayer structures with ease. This paper aptly characterizes the linear (traditional) F-mixing sticker and the spiral F-mixing sticker to compare those against the F-mixers' performance described in the previously published studies. Upon characterization, the mixer is applied to mix primary and secondary antibodies on a micropatterned microdot array to exemplify its ability to distribute an even mix throughout the channel. As a

final testament to its superior design, the same experiment was conducted and compared against the performance of a T-mixer. The results demonstrated the promising performance of the stickers being able to mix not only at a range of Reynolds numbers, but also at disparate volumes, lending this technology to limitless applications.

For decades, classic microfluidic mixers have traditionally been difficult to manufacture and integrate into microfluidic devices. To our knowledge, this paper was the first introduction to a new paradigm of universal sticker microfluidic mixers that are simple to manufacture and flexible, and adapt to any application via their ability to retrofit pre-existing microfluidics and work reliably over a wide range of Reynolds numbers. The revamped F-mixers mirrored the CFD simulation and were able to mix highly disparate volumes despite being tested over three different magnitudes of Reynolds numbers. Mixing primary and secondary antibodies showcased this technology's limitless potential for different applications, as well as confirming its ability to outperform a T-mixer. The mixer's strong performance opens the doors for sticker microfluidics to change the way we think about microfluidics as a whole.

Our dry-film sticker microfluidics could find broad use in basic biomedical research utilizing microfluidics. While several implementations of double-coated adhesive tape layers have been used as interfaces for sensors, surprisingly few implementations have been done on biologically active surfaces. For example, our approach can create simple microfluidic channels that attach to biologically active micropatterned surfaces that are often used in hematology research.[47–49] Moreover, our pre-mixer can be added to existing devices to enable integrated on-chip re-coagulation of whole blood by mixing whole blood with $CaCl_2$, especially as our mixer is agnostic to the flow speed or mixing ratio. Such an approach would replace the existing two chip approaches[15–50] and solve the issue of recalcified blood clotting in upstream syringes/tubes. As our bonding process is non-destructive, it can also simplify point-of-care assay assembly by enabling sticker microfluidics to be added on top of microspotting and lyophilization of key reagents on simple flat substrates.[51,52]

More broadly, the ability to add up- and down-stream processes to existing microfluidics could prove useful in a variety of settings. As many point-of-care devices require some sample preparation before use, upstream processes to dilute samples or extract biomarkers may help such devices begin to bridge the translational gap by making them easier to use. Our dry film sticker technology could also be adapted to add inexpensive commercially available upstream filters to existing point-of-care devices and to enable them to process more complex patient samples such as blood, urine, sweat, and saliva. Traditional approaches of sample processing in microfluidics consist of separate systems that are either designed with the rest of the point-of-care devices or a separate entity of its own that gets connected via tubing.[53] The seamless integration to existing microfluidics and reduction in the overall surface area frame the sticker microfluidic as an attractive option to continue to innovate better point-of-care microfluidics.

For microphysiological systems on a chip, our dry film sticker approach could open up the option of integrating upstream bubble traps to help protect long-term cell cultures from catastrophic damage due to bubbles. Many bubble traps have been designed to be incorporated within the microfluidic.[54] This would save from having to redesign the microfluidic to include a bubble trap, in the case that the case of air bubbles was not identified until after the microfluidic platform was tested. The modularly added bubble trap to the existing microfluidic platform could then be loaded with cells. The weeks and months saved from having another mold made in the cleanroom to address this would significantly reduce the overall amount of time spent troubleshooting.

Sticker microfluidics offer many remarkable advantages to traditional microfluidics. The seamless incorporation into existing microfluidics, sticker or traditional, allows for the endless modular customization of microfluidics. The sticker will find many uses not only in integration, but also when used with surfaces that need to be preserved without the need for tedious manufacturing steps. The benefits are infinite in sample preparation, mixing, and manipulation of fluids regardless of the application at hand.

SUPPLEMENTARY MATERIAL

See the supplementary material for the video of the antibody mixing and fluorescently tagging microdot surface, alternative designs for the linear F-mixer, additional simulations for the linear and spiral F-mixers that retrofit to an existing microfluidic, experimental data of the spiral F-mixer vs short and long T-mixers for antibody mixing, comparisons of mixing at different Reynolds numbers for the spiral F-mixer vs short and long T-mixers, and an analysis on the intervariable alignment of microfluidic layers between separate users.

ACKNOWLEDGMENTS

The financial support was provided by NIH R01 (Grant No. HL155330) and NIH K25 (Grant No. HK141636).

AUTHOR DECLARATIONS

Conflict of Interest

The authors have no conflicts to disclose.

Author Contributions

P.D. designed CAD for the microfluidics, ran simulations on the CAD, fabricated microfluidic devices, ran experiments, and drafted manuscript. O.O. assisted with running antibody experiments, analyzing data, creating figures, and helped draft manuscript. M.E.F. developed the Matlab code and analyzed antibody experiments. C.A.L. assisted with the fabrication of microfluidic devices and running experiments. A.D. assisted with fabrication and preparation of microfluidic devices as well as running experiments. P.D. assisted with the design of the microfluidics and characterization of microfluidics. A.R. assisted with the design of the microfluidics and characterization of microfluidics. L.S. assisted with antibody experiments. D.R.M. oversaw the microfluidic design and analysis, and revised the manuscript.

P. Delgado: Conceptualization (equal); Data curation (equal); Formal analysis (equal); Methodology (equal); Software (equal);

Validation (equal); Visualization (equal); Writing – original draft (equal); Writing – review & editing (equal). **O. Oshinowo:** Data curation (supporting); Formal analysis (supporting); Software (supporting); Visualization (supporting); Writing – review & editing (supporting). **M. E. Fay:** Formal analysis (supporting); Software (lead). **C. A. Luna:** Data curation (supporting). **A. Dissanayaka:** Data curation (supporting). **P. Dorbala:** Data curation (supporting). **A. Ravindran:** Data curation (supporting). **L. Shen:** Conceptualization (equal); Data curation (supporting); Formal analysis (equal); Funding acquisition (equal); Investigation (equal); Methodology (equal); Visualization (supporting); Writing – original draft (equal); Writing – review & editing (equal). **D. R. Myers:** Conceptualization (equal); Data curation (supporting); Formal analysis (equal); Funding acquisition (equal); Investigation (equal); Methodology (equal); Visualization (supporting); Writing – original draft (equal); Writing – review & editing (equal).

DATA AVAILABILITY

The data that support the findings of this study are available from the corresponding author upon reasonable request.

REFERENCES

[1]M. A. Dineva, L. MahiLum-Tapay, and H. Lee, "Sample preparation: A challenge in the development of point-of-care nucleic acid-based assays for resource-limited settings," Analyst **132**, 1193–1199 (2007).

[2]J. J. Waggoner and B. A. Pinsky, "Comparison of automated nucleic acid extraction methods for the detection of cytomegalovirus DNA in fluids and tissues," PeerJ **2**, e334 (2014).

[3]D.-H. Kuan, C.-C. Wu, W.-Y. Su, and N.-T. Huang, "A microfluidic device for simultaneous extraction of plasma, red blood cells, and on-chip white blood cell trapping," Sci. Rep. **8**, 15345 (2018).

[4]J. H. Imran and J. K. Kim, "A nut-and-bolt microfluidic mixing system for the rapid labeling of immune cells with antibodies," Micromachines **11**, 280 (2020).

[5]J.-M. Lim *et al.*, "Ultra-high throughput synthesis of nanoparticles with homogeneous size distribution using a coaxial turbulent jet mixer," ACS Nano **8**, 6056–6065 (2014).

[6]A. Mukherjee *et al.*, "Lipid-polymer hybrid nanoparticles as a next-generation drug delivery platform: State of the art, emerging technologies, and perspectives," Int. J. Nanomed. **14**, 1937–1952 (2019).

[7]I. V. Zhigaltsev *et al.*, "Bottom-up design and synthesis of limit size lipid nanoparticle systems with aqueous and triglyceride cores using millisecond microfluidic mixing," Langmuir **28**, 3633–3640 (2012).

[8]V. Mengeaud, J. Josserand, and H. H. Girault, "Mixing processes in a zigzag microchannel: Finite element simulations and optical study," Anal. Chem. **74**, 4279–4286 (2002).

[9]W. Raza, S.-B. Ma, and K.-Y. Kim, "Multi-objective optimizations of a serpentine micromixer with crossing channels at low and high Reynolds numbers," Micromachines **9**, 110 (2018).

[10]G. Salieb-Beugelaar, D. Gonçalves, M. Wolf, and P. Hunziker, "Microfluidic 3D helix mixers," Micromachines **7**, 189 (2016).

[11]R. H. Liu *et al.*, "Passive mixing in a three-dimensional serpentine microchannel," J. Microelectromech. Syst. **9**, 190–197 (2000).

[12]D. S. Kim, S. H. Lee, T. H. Kwon, and C. H. Ahn, "A serpentine laminating micromixer combining splitting/recombination and advection," Lab Chip **5**, 739–747 (2005).

[13]S. M. Scott and Z. Ali, "Fabrication methods for microfluidic devices: An overview," Micromachines **12**, 319 (2021).

[14]A.-G. Niculescu, C. Chircov, A. C. Bîrcă, and A. M. Grumezescu, "Fabrication and applications of microfluidic devices A review," Int. J. Mol. Sci. **22**, 2011 (2021).

[15]M. Lehmann *et al.*, "On-chip recalcification of citrated whole blood using a microfluidic herringbone mixer," Biomicrofluidics **9**, 064106 (2015).

[16]A. P. Kuo *et al.*, "High-precision stereolithography of biomicrofluidic devices," Adv. Mater. Technol. **4**, 1800395 (2019).

[17]Y. He, Y. Wu, J.-Z. Fu, Q. Gao, and J.-J. Qiu, "Developments of 3D printing microfluidics and applications in chemistry and biology: A review," Electroanalysis **28**, 1658–1678 (2016).

[18]B. Levaché, A. Azioune, M. Bourrel, V. Studer, and D. Bartolo, "Engineering the surface properties of microfluidic stickers," Lab Chip **12**, 3028–3031 (2012).

[19]J. Greer, S. O. Sundberg, C. T. Wittwer, and B. K. Gale, "Comparison of glass etching to xurography prototyping of microfluidic channels for DNA melting analysis," J. Micromech. Microeng. **17**, 2407 (2007).

[20]A. Neuville *et al.*, "Xurography for microfluidics on a reactive solid," Lab Chip **17**, 293–303 (2017).

[21]S.-G. Jeong, S.-H. Lee, C.-H. Choi, J. Kim, and C.-S. Lee, "Toward instrument-free digital measurements: A three-dimensional microfluidic device fabricated in a single sheet of paper by double-sided printing and lamination," Lab Chip **15**, 1188–1194 (2015).

[22]J. I. Martínez-López, M. Mojica, C. A. Rodríguez, and H. R. Siller, "Xurography as a rapid fabrication alternative for point-of-care devices: Assessment of passive micromixers," Sensors **16**, 705 (2016).

[23]L. C. Gerber, H. Kim, and I. H. Riedel-Kruse, "Microfluidic assembly kit based on laser-cut building blocks for education and fast prototyping," Biomicrofluidics **9**, 064105 (2015).

[24]G. A. Cooksey and J. Atencia, "Pneumatic valves in folded 2D and 3D fluidic devices made from plastic films and tapes," Lab Chip **14**, 1665–1668 (2014).

[25]L. E. Stallcop *et al.*, "Razor-printed sticker microdevices for cell-based applications," Lab Chip **18**, 451–462 (2018).

[26]D. Bartolo, G. Degré, P. Nghe, and V. Studer, "Microfluidic stickers," Lab Chip **8**, 274–279 (2008).

[27]I. T. Neckel *et al.*, "Development of a sticker sealed microfluidic device for *in situ* analytical measurements using synchrotron radiation," Sci. Rep. **11**, 23671 (2021).

[28]D. A. Bartholomeusz, R. W. Boutte, and J. D. Andrade, "Xurography: Rapid prototyping of microstructures using a cutting plotter," J. Microelectromech. Syst. **14**, 1364–1374 (2005).

[29]P. Nath *et al.*, "Rapid prototyping of robust and versatile microfluidic components using adhesive transfer tapes," Lab Chip **10**, 2286–2291 (2010).

[30]N. Chang *et al.*, "Low cost 3D microfluidic chips for multiplex protein detection based on photonic crystal beads," Lab Chip **18**, 3638–3644 (2018).

[31]D. Patko *et al.*, "Microfluidic channels laser-cut in thin double-sided tapes: Cost-effective biocompatible fluidics in minutes from design to final integration with optical biochips," Sens. Actuators B **196**, 352–356 (2014).

[32]J. Kim, R. Surapaneni, and B. K. Gale, "Rapid prototyping of microfluidic systems using a PDMS/polymer tape composite," Lab Chip **9**, 1290–1293 (2009).

[33]P. K. Yuen and V. N. Goral, "Low-cost rapid prototyping of flexible microfluidic devices using a desktop digital craft cutter," Lab Chip **10**, 384–387 (2010).

[34]X. Lai *et al.*, "Sticker microfluidics: A method for fabrication of customized monolithic microfluidics," ACS Biomater. Sci. Eng. **5**, 6801–6810 (2019).

[35]P. Khashayar *et al.*, "Rapid prototyping of microfluidic chips using laser-cut double-sided tape for electrochemical biosensors," J. Braz. Soc. Mech. Sci. Eng. **39**, 1469–1477 (2017).

[36]M. A. Unger, H. P. Chou, T. Thorsen, A. Scherer, and S. R. Quake, "Monolithic microfabricated valves and pumps by multilayer soft lithography," Science **288**, 113–116, (2000).

[37]J. Cha *et al.*, "A highly efficient 3D micromixer using soft PDMS bonding," J. Micromech. Microeng. **16**, 1778 (2006).

[38]S. Satyanarayana, R. N. Karnik, and A. Majumdar, "Stamp-and-stick room-temperature bonding technique for microdevices," J. Microelectromech. Syst. **14**, 392–399 (2005).

[39]N. Y. Lee and B. H. Chung, "Novel poly(dimethylsiloxane) bonding strategy via room temperature 'chemical gluing,'" Langmuir **25**, 3861–3866 (2009).
[40]L. Martynova *et al.*, "Fabrication of plastic microfluid channels by imprinting methods," Anal. Chem. **69**, 4783–4789 (1997).
[41]P.-O. Gendron, F. Avaltroni, and K. J. Wilkinson, "Diffusion coefficients of several rhodamine derivatives as determined by pulsed field gradient-nuclear magnetic resonance and fluorescence correlation spectroscopy," J. Fluoresc. **18**, 1093–1101 (2008).
[42]O. Oshinowo *et al.*, "Significant differences in single-platelet biophysics exist across species but attenuate during clot formation," Blood Adv. **5**, 432–437 (2021).
[43]D. R. Myers *et al.*, "Single-platelet nanomechanics measured by high-throughput cytometry," Nat. Mater. **16**, 230–235 (2017).
[44]S. van der Walt *et al.*, "scikit-image: Image processing in python," PeerJ **2**, e453 (2014).
[45]N. Herzog, A. Johnstone, T. Bellamy, and N. Russell, "Characterization of neuronal viability and network activity under microfluidic flow," J. Neurosci. Methods **358**, 109200 (2021).
[46]E. E. Edwards, K. G. Birmingham, M. J. O'Melia, J. Oh, and S. N. Thomas, "Fluorometric quantification of single-cell velocities to investigate cancer metastasis," Cell Syst. **7**, 496–509.e6 (2018).
[47]K. B. Neeves and S. L. Diamond, "A membrane-based microfluidic device for controlling the flux of platelet agonists into flowing blood," Lab Chip **8**, 701–709 (2008).
[48]T. V. Colace, P. F. Fogarty, K. A. Panckeri, R. Li, and S. L. Diamond, "Microfluidic assay of hemophilic blood clotting: Distinct deficits in platelet and fibrin deposition at low factor levels," J. Thromb. Haemostasis **12**, 147–158 (2014).
[49]R. M. Schoeman, M. Lehmann, and K. B. Neeves, "Flow chamber and microfluidic approaches for measuring thrombus formation in genetic bleeding disorders," Platelets **28**, 463–471 (2017).
[50]S. Zhu *et al.*, "In microfluidico: Recreating *in vivo* hemodynamics using miniaturized devices," Biorheology **52**, 303–318 (2016).
[51]M. F. Templin *et al.*, "Protein microarray technology," Trends Biotechnol. **20**, 160–166 (2002).
[52]S. Ghosh and C. H. Ahn, "Lyophilization of chemiluminescent substrate reagents for high-sensitive microchannel-based lateral flow assay (MLFA) in point-of-care (POC) diagnostic system," Analyst **144**, 2109–2119 (2019).
[53]E. K. Sackmann, A. L. Fulton, and D. J. Beebe, "The present and future role of microfluidics in biomedical research," Nature **507**, 181–189 (2014).
[54]X. He, B. Wang, J. Meng, S. Zhang, and S. Wang, "How to prevent bubbles in microfluidic channels," Langmuir **37**, 2187–2194 (2021).